Neutron Shell Structure in ^{125}Sn by (d, p) and $(\alpha, {}^3\mathrm{He})$ Reactions*

C. R. Bingham
The University of Tennessee, Knoxville, Tennessee 37916
Oak Ridge National Laboratory, Oak Ridge, Tennessee 37830

D. L. Hillis
The University of Tennessee, Knoxville, Tennessee 37916

(Received 16 October 1972; revised manuscript received 9 April 1973)

Differential cross sections for ^{124}Sn(d, p) at 33.3 MeV were measured in 5° increments from 12.5 to 47.5° lab. The resolution was about 30 keV full width at half maximum. The $(\alpha, {}^3\mathrm{He})$ spectra with ≈ 55-keV resolution were obtained at 15 and 20° lab with 65.7-MeV α particles. Distorted-wave calculations were made, allowing the assignment of l values, some of which were not made in earlier neutron-transfer studies. Spin assignments and spectroscopic factors were obtained in accordance with the shell model. Consistent spectrocopic factors were obtained from the (d, p) and $(\alpha, {}^3\mathrm{He})$ reactions. Sums of spectroscopic factors and centers of gravity are presented for the levels observed and are compared with the results of pairing theory. Essentially all the neutron strength remaining in the neutron shell between $N = 50$ and $N = 82$ was located. Most of the strength in the $2f_{7/2}$, $3p_{3/2}$, and $1h_{9/2}$ levels of the next major shell was located.

I. INTRODUCTION

In a recent study of the neutron shell structure of the Zr isotopes[1,2] it was shown that the (d,p) and $(\alpha, {}^3\mathrm{He})$ reactions complement each other in the study of single-particle structure of nuclei. Transitions involving a low-l transfer are the strongest in the (d,p) reaction while those involving an l transfer of 4–6 are strongest in the $(\alpha, {}^3\mathrm{He})$ reaction.

The Sn isotopes have been previously studied by low-energy (d,p) and (d, t) reactions.[3-6] Still there was considerable uncertainty, and in some cases, complete lack of knowledge about those subshells populated by high-l transfers, i.e., the $1h_{11/2}$, $2f_{7/2}$, and $1h_{9/2}$ subshells. Consequently, the present study was initiated to obtain a more complete picture of the neutron shell structure of ^{125}Sn. In order to enhance the population of the higher spin states, a deuteron bombarding energy

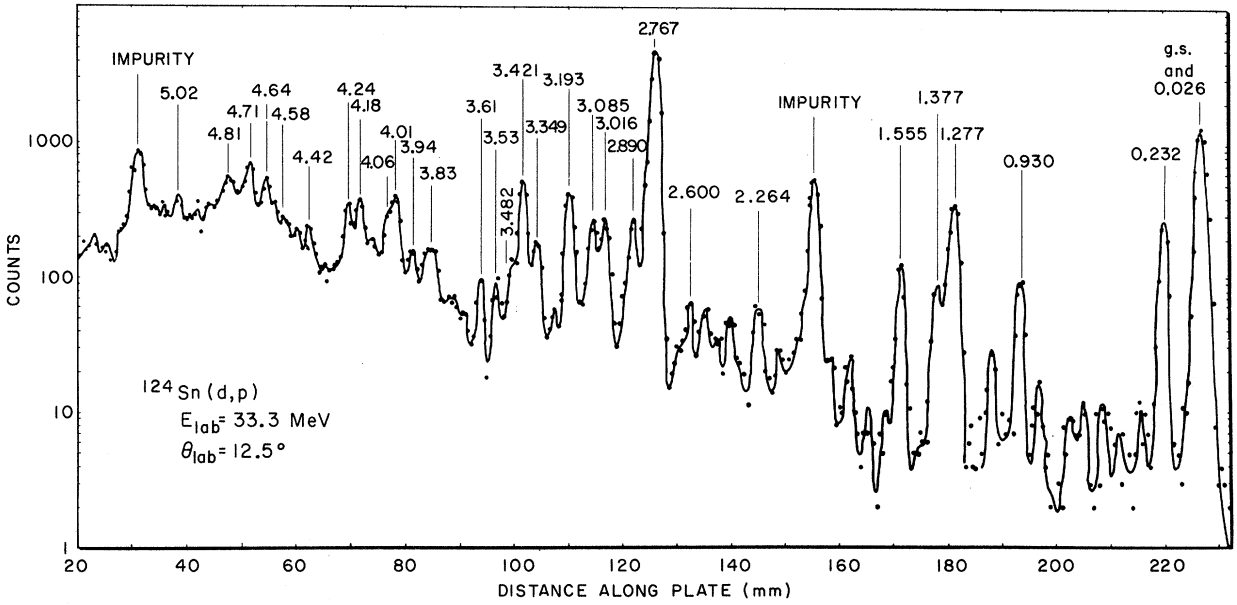

FIG. 1. The ^{124}Sn(d, p) spectrum at 12.5° lab. The excitation energies of the residual states are given for the prominent transitions, and peaks from light impurities are identified.

more than twice the bombarding energy for the earlier experiments was used. Since optical-model parameters describing the elastic scattering of 34-MeV deuterons[7] and 30- and 40-MeV protons[8] are available, a bombarding energy near 34 MeV was selected. The bombarding energy for the $(\alpha, {}^3\mathrm{He})$ studies was chosen to coincide with earlier elastic and inelastic scattering studies[9] and with $^{116}\mathrm{Sn}(\alpha, {}^3\mathrm{He})$ studies.[10]

II. EXPERIMENTAL DETAILS

The deuterons and α particles were accelerated to 33.3 and 65.7 MeV, respectively, by the Oak Ridge isochronous cyclotron. The reactions were studied in the broad-range spectrograph facility, with the outgoing protons and ^{3}He being detected in 50-μm-thick nuclear emulsions in the focal plane. The emulsions were subsequently scanned in $\frac{1}{2}$-mm strips.

The ^{124}Sn target, furnished by the cyclotron laboratory, was 0.6 mg/cm^2 thick and was ~99% isotopically pure. The uncertainty in target thickness is about 15%. This is the principal contribution to the over-all uncertainty of the absolute cross sections which is estimated to be ±20%.

The $^{124}\mathrm{Sn}(d,p)$ spectrum at 12.5° is shown in Fig. 1. Peaks due to light impurities are identified in the figure. The full width at half maximum for the single-level peaks is typically 30 keV. The experimental uncertainties on the excitation energies are believed to be about 5–10 keV. The ground-state peak is a doublet which was previously separated by Nealy and Sheline.[5]

The $^{124}\mathrm{Sn}(\alpha, {}^3\mathrm{He})$ spectrum at 20° is shown in Fig. 2. The statistics were insufficient to study the low-l transfers, but transitions to the higher spin states are clearly observable and statistical uncertainties are less than 10% for most cross sections that were analyzed. The resolution in the ^{3}He spectra is about 55 keV and hence some states resolved in the proton spectra were not resolved here. The largest peak in the $(\alpha, {}^3\mathrm{He})$ spectrum is the ground state which is populated by an $l=5$ transition. Cross sections for the $l=3$ transitions around 3–4 MeV are fairly large, but the $l=0$ and $l=1$ transitions are not observable in the present ^{3}He spectra. The peaks near 5 MeV are fairly large and are presumably due to transitions to the $1h_{9/2}$ subshell. Since the distorted-wave theory predicts these grossly different cross sections for (d,p) and $(\alpha, {}^3\mathrm{He})$ for all the l transfers involved, one obtains added confidence in spin assignments which give consistent spectroscopic factors from the two reactions.

Angular distributions of the proton groups were obtained in 5° increments from 12.5 to 47.5° lab for comparison with distorted-wave predictions. Since the $(\alpha, {}^3\mathrm{He})$ angular distributions are not very characteristic of the l transfer,[10] particularly for the higher spin states, the ^{3}He spectra were measured at only 15 and 20° lab.

III. DISTORTED-WAVE ANALYSIS

Distorted-wave calculations were made with the program JULIE[11] for both the (d,p) and $(\alpha, {}^3\mathrm{He})$

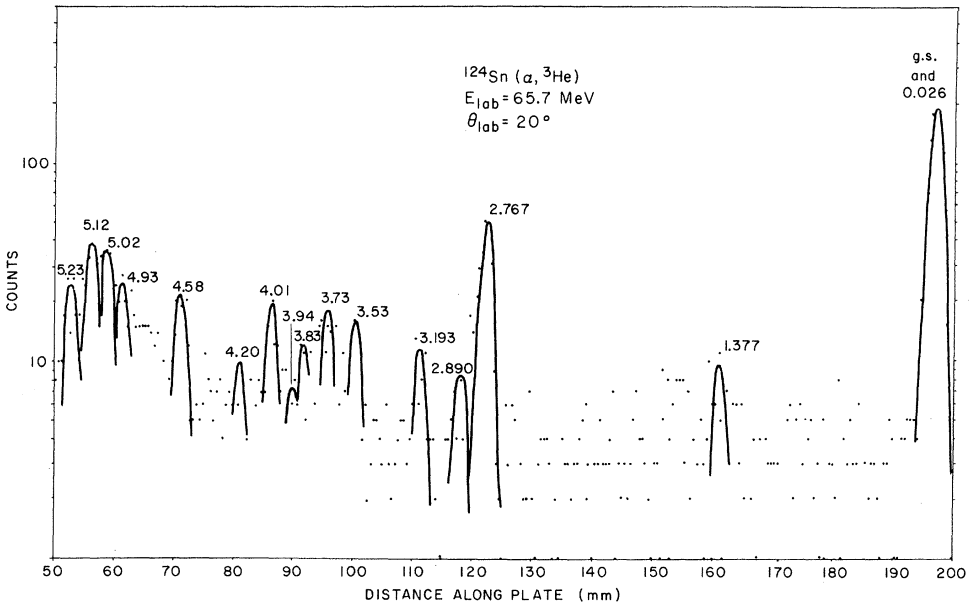

FIG. 2. The $^{124}\mathrm{Sn}(\alpha, {}^3\mathrm{He})$ spectrum at 20° lab. The excitation energies, shown for the prominent transitions, were taken from $^{124}\mathrm{Sn}(d,p)$.

TABLE I. Optical-model parameters used in the distorted-wave calculations.

Particle	V_0 (MeV)	W_0 (MeV)	W_D (MeV)	V_s (MeV)	r_0 (fm)	a_0 (fm)	r_0' (fm)	a_0' (fm)	r_s (fm)	a_s (fm)	r_c (fm)	Reference
d	98.95	0.0	15.3	7.00	1.113	0.814	1.25	0.848	r_0	a_0	1.30	7
p	49.93	4.52	4.94	6.04	1.16	0.75	1.37	0.63	1.064	0.738	1.25	8
α	100	53.74			1.352	0.667	r_0	a_0			1.40	9
^{3}He	196.9	17.37			1.04	0.811	1.60	0.797			1.40	12

cross sections. The distorted-wave cross section is given by

$$\frac{d\sigma}{d\Omega} = \frac{NR}{2s+1}\,\frac{2J_f+1}{2J_i+1}\,S\sigma^{(\theta)}_{\text{JULIE}},$$

where J_i and J_f are the spins of the target and residual nuclei, respectively; s $(=\frac{1}{2})$ is the spin of the stripped neutron; S is the spectroscopic factor; and NR accounts for the overlap of the ingoing particle and the outgoing particle-neutron system, as well as the strength of the interaction causing the transition. For the (d,p) calculations a value of $NR=3.30$ was used.[2] The value of $NR=92.1$ used here for the $(\alpha, {}^3\text{He})$ calculations was obtained empirically in previous work.[12]

The distorted-wave calculation for the (d,p) cross sections employed nonlocal potentials[13] for the ingoing and outgoing channels and finite-range effects in the local energy approximation.[14] No radial cutoffs were used. The ranges used for the deuteron and proton channels were 0.54 and 0.85 fm, respectively. The range of the interaction was taken to be 1.54 fm. The nonlocality and finite-range corrections were made by multiplying the local zero-range form factor by appropriate corrective functions.[13,14] The local zero-range form factor is the radial bound-state wave function for the stripped neutron. It was taken as the solution of Schrödinger's equation with a Woods-Saxon potential with a spin-orbit term of the Thomas form having $r_0=1.24$ fm, $a=0.65$ fm, $r_{0s}=1.14$ fm, $a_s=0.65$ fm, $\lambda=25$, and a well depth adjusted to give an eigenvalue equal to the binding energy of the transferred neutron.

The elastic scattering of 34.4-MeV deuterons from several targets has been studied.[7] In Ref. 7 an average potential, which is a function of A and Z, was developed. This average potential was used in the present calculation to obtain the wave function for the ingoing deuteron. The parameters are listed on the first line of Table I.

The proton energies varied from 31 to 36.5 MeV. The potential for the proton channel was obtained by interpolation between the potentials which fit the elastic scattering cross section and polarization data at 30 and 40 MeV.[8] The parameters near mid-range (~33.7 MeV) are listed in Table I. The parameters for the other energies were very similar.

The $(\alpha, {}^3\text{He})$ calculations were made in zero range with local potentials. The optical potentials for α and ^{3}He particles are somewhat ambiguous and effects similar to the effects of nonlocality and finite range can be produced by choosing α potentials with deeper absorptive wells. Hence, the α and ^{3}He potentials were chosen to be similar to those used in previous $(\alpha, {}^3\text{He})$ and $({}^3\text{He}, \alpha)$ analyses[12,15] to fit measured angular distributions. The ^{3}He potential was obtained from the scattering of 51-MeV ^{3}He from ^{92}Zr,[12] but the ^{3}He potential does not have a large A dependence.[16] The α potential was selected from the large number of ambiguous potentials which fit the elastic scattering of 65-MeV α particles from ^{116}Sn.[9] The α and ^{3}He

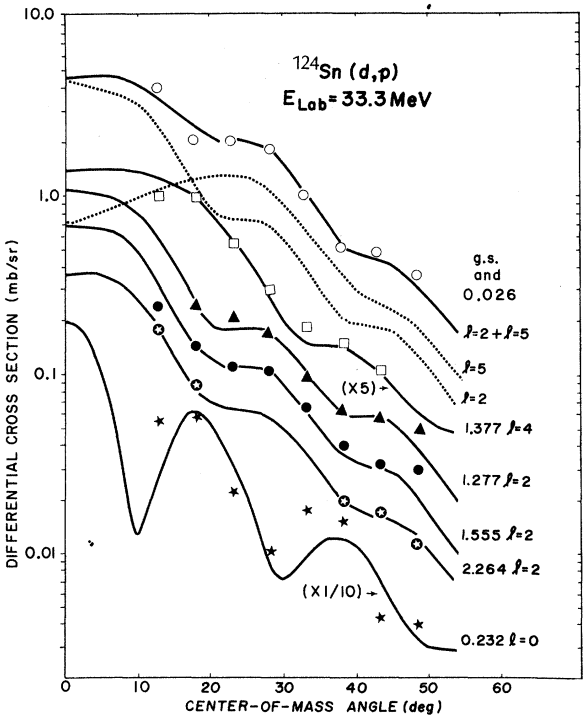

FIG. 3. Experimental angular distributions of ^{124}Sn-(d,p) for the transitions to the major shell below $N=82$ in comparison with the distorted-wave calculations.

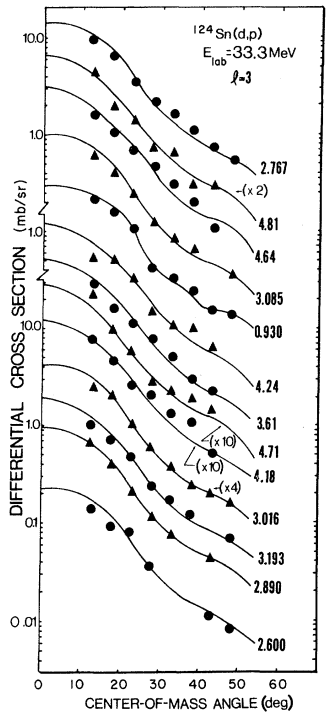

FIG. 4. Experimental angular distributions for the l =3 transitions in ^{124}Sn(d,p) in comparison with the distorted-wave calculations.

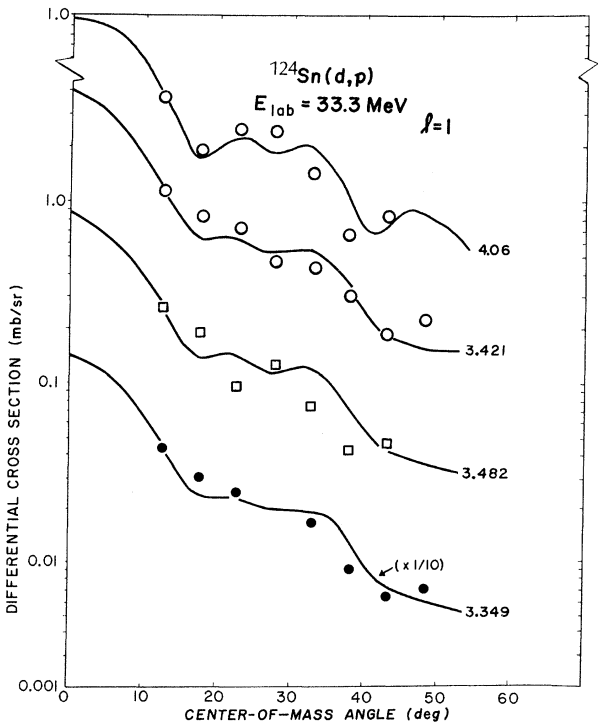

FIG. 5. Experimental angular distributions for the l =1 transitions in ^{124}Sn(d,p) in comparison with the distorted-wave calculations.

optical-model parameters used are also listed in Table I.

IV. RESULTS AND DISCUSSION

Preliminary distorted-wave analysis of the (d,p) and $(\alpha, {}^3\mathrm{He})$ cross sections gave $(\alpha, {}^3\mathrm{He})$ results in agreement with the results of the (d,p) measurements at 15 MeV [3] and (d,p) results that were somewhat larger. It was assumed that a systematic error had occurred and the (d,p) cross sections were multiplied by 0.8 to achieve agreement. The resulting ^{124}Sn(d,p) differential cross sections are compared with the distorted-wave predictions in Figs. 3–6. The corresponding excitation energies, spin assignments, and spectroscopic factors are listed in Table II. The spectroscopic factors from the $(\alpha, {}^3\mathrm{He})$ reaction as well as those obtained from (d,p) at 15 MeV [3] are also given in Table II. Due to the dominance of the large-l transfers in the $(\alpha, {}^3\mathrm{He})$ spectrum and the relatively poor statistics in the ^{3}He spectra it was not possible to obtain spectroscopic factors for the $l=0$ to $l=2$ and the weak $l=3$ transitions. In a few

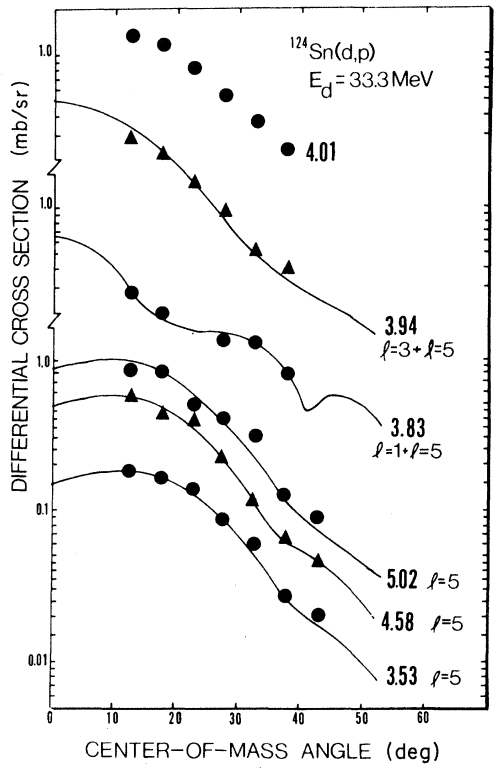

FIG. 6. Experimental angular distributions for groups containing l =5 transitions. The lower three distributions were treated as pure l =5 transitions. The next two were treated as doublets. Agreement between (d,p) and $(\alpha, {}^3\mathrm{He})$ could not be achieved for the 4.01-MeV group using just two l values; it presumably contains at least three states.

cases where states were not resolved in the $(\alpha, {}^3\mathrm{He})$ spectrum, the component due to the lower-l transfer was subtracted and the spectroscopic factor for the higher spin state was then deduced for comparison. Also, two peaks were treated as doublets in both the (d,p) and $(\alpha, {}^3\mathrm{He})$ spectra in order to obtain consistent spectroscopic factors from the two reactions. The state at 4.01 MeV could not be adequately fit with a two-component curve which would agree with the $(\alpha, {}^3\mathrm{He})$ results. This group probably contains at least three states and is shown in Fig. 6 without a theoretical prediction.

The low-lying levels which correspond to stripping the neutron into the $N=50-82$ shell are shown in Fig. 3. The ground-state peak contained both the $1h_{11/2}$ ground state and the $2d_{3/2}$ state at 0.026 MeV.[5] The $h_{11/2}$ part was obtained from the $(\alpha, {}^3\mathrm{He})$ results and the $d_{3/2}$ part deduced. Both the $l=2$ and $l=5$ components are shown in Fig. 3. The $h_{11/2}$ spectroscopic factor was not obtained in the lower-energy work.[3] The $l=2$ states between 1.27 and 2.27 MeV can be either $d_{3/2}$ or $d_{5/2}$ states; they are tentatively given $(\frac{5}{2}^+)$ assignments. Reference 3 did not report the $(1g_{7/2})$ level at 1.377 MeV and made a tentative assignment of $s_{1/2}$ for the state near 2.27 MeV.

The angular distributions for the $2f_{7/2}$ transfers are shown in Fig. 4. The spectroscopic factors for the states near 2.60, 3.19, 3.61, and 4.81 MeV agree fairly well with the corresponding results from Ref. 3, and the sum of the spectroscopic factors for the states 4.18 and 4.24 MeV agree with the result of Schneid, Prakash, and Cohen[3] for the group at 4.20 MeV. Spin assignments and spectroscopic factors were not reported in Ref. 3 for the states at 0.94, 2.76, 3.00, 4.67, and 4.73 MeV in spite of the fact that the 2.76-MeV transition was the strongest in their spectrum. The spectroscopic factors given in square brackets in

TABLE II. Excitation energies, spins, and spectroscopic factors in comparison with the results from ^{124}Sn(d,p) at 15 MeV.

Present results				^{124}Sn(d,p) (15 MeV) [a]			Present results				^{124}Sn(d,p) (15 MeV) [a]		
E^* (MeV) [b]	nl_j	$S_{d,p}$	$S_{\alpha,{}^3\mathrm{He}}$	E^* (MeV)	nl_j	S	E^* (MeV) [b]	nl_j	$S_{d,p}$	$S_{\alpha,{}^3\mathrm{He}}$	E^* (MeV)	nl_j	S
0.0	$1h_{11/2}$	0.42	0.41 [c]	0.0	$1h_{11/2}$		3.73	$(1h_{9/2})$	f	0.05			
0.026 [d]	$2d_{3/2}$	0.44	c	0.026	$2d_{3/2}$	0.34	3.83	$(3p_{3/2}, 1h_{9/2})$	0.10, 0.02	0.10, [g] 0.02	3.85	$(2f_{7/2})$	0.078
0.232	$3s_{1/2}$	0.33		0.22	$3s_{1/2}$	0.25							
0.930	$(2f_{7/2})$	0.015		0.94	$[2f_{7/2}]$ [e]	[0.012] [e]	3.94	$(2f_{7/2}, 1h_{9/2})$	0.02, 0.01	0.01, [h] 0.01			
1.277	$2d_{(5/2)}$	0.07		1.27	$(2d_{5/2})$	0.039							
1.377	$1g_{7/2}$	0.038	0.056				4.01	$(1h_{9/2})$	i	0.06	4.03	$(3p_{3/2})$	0.24
1.555	$2d_{(5/2)}$	0.04		1.56	$(2d_{5/2})$	0.023	4.06	$(3p_{3/2})$	0.14				
2.264	$(2d_{5/2})$	0.019		2.27	$(3s_{1/2})$	0.009	4.18	$(2f_{7/2})$	0.04	0.06	4.20	$(2f_{7/2})$	0.071
2.600	$(2f_{7/2})$	0.010		2.59	$(2f_{7/2})$	0.011	4.24	$(2f_{7/2})$	0.04				
2.767	$2f_{7/2}$	0.54	0.54	2.76	$[2f_{7/2}]$ [e]	[0.58] [e]	4.42						
2.890	$(2f_{7/2})$	0.032					4.58	$(1h_{9/2})$	0.08	0.11	4.55		
3.016	$2f_{7/2}$	0.04		3.00	$[2f_{7/2}]$ [e]	[0.026] [e]	4.64	$(2f_{7/2})$	0.09		4.67	$[2f_{7/2}]$ [e]	[0.039] [e]
3.085	$2f_{7/2}$	0.04		3.07	$(3p_{3/2})$	0.036	4.71	$(2f_{7/2})$	0.08		4.73	$[2f_{7/2}]$ [e]	[0.083] [e]
3.193	$2f_{7/2}$	0.067	0.059	3.18	$(2f_{7/2})$	0.058	4.81	$(2f_{7/2})$	0.10		4.83	$(2f_{7/2})$	0.059
3.349	$(3p_{3/2})$	0.14		3.35	$(2f_{7/2})$	0.062	4.93	$(1h_{9/2})$	f	0.11			
3.421	$3p_{3/2}$	0.36		3.42	$(3p_{3/2})$	0.34	5.02	$(1h_{9/2})$	0.13	0.15			
3.482	$3p_{3/2}$	0.08					5.12	$(1h_{9/2})$	f	0.15			
3.53	$(1h_{9/2})$	0.04	0.04	3.53	$(3p_{3/2})$	0.042	5.23	$(1h_{9/2})$	f	0.11			
3.61	$(2f_{7/2})$	0.02		3.63	$(2f_{7/2})$	0.021							

[a] See Ref. 3.

[b] Excitation energies taken from ^{124}Sn(d,p) except for the few cases where only $(\alpha, {}^3\mathrm{He})$ spectroscopic factors are given.

[c] The angular distribution was corrected for the $2d_{3/2}$ component at 0.026 MeV before analysis as $1h_{11/2}$.

[d] Energy from Ref. 5.

[e] These quantities were not reported in Ref. 3, but were deduced from their data in the present work.

[f] The spectroscopic factor was not calculated from (d,p) data because a single peak was not dominant in the (d,p) spectra. There were sufficient counts within an $(\alpha, {}^3\mathrm{He})$ resolution width to be consistent with the $(\alpha, {}^3\mathrm{He})$ interpretation.

[g] The $l=1$ component was small and was subtracted before analysis as an $l=5$.

[h] The $l=3$ component was small and was subtracted before analysis as an $l=5$.

[i] The angular distribution for the peak at 4.01 MeV is similar to an $l=5$ distribution but the strength is about 3 times as large as is indicated by the $(\alpha, {}^3\mathrm{He})$.

TABLE III. Parameters used to calculated the quasiparticle energies E_j and the nonoccupation probabilities U_j^2 from pairing theory (in MeV) (see Ref. 17).

Set	λ	Δ	$\epsilon_{5/2}$	$\epsilon_{7/2}$	$\epsilon_{1/2}$	$\epsilon_{3/2}$	$\epsilon_{11/2}$
I	2.79	1.03	0.015	0.805	1.282	2.740	2.485
II	2.79	1.44[a]	0.015	0.805	1.282	2.740	2.485
III	2.79	1.44[a]	0.015	0.805	2.0	2.740	2.485

[a] Taken from Ref. 3.

Table II were obtained by the scaling of neighboring $l=3$ spectroscopic factors that were reported with the ratio of the peak cross sections. In each of these cases the spectroscopic factors so deduced agree well with those obtained in the present work. Also, the angular distributions pictured for these states in Ref. 3 do not appear to be inconsistent with the $f_{7/2}$ assignments. A tentative new $l=3$ transition is reported at 2.89 MeV and an $l=3$ component was included in the description of the multiplet peak at 3.94 MeV. The peak near 3.08 MeV reported as $(3p_{3/2})$ in Ref. 3 appears to be due to an $l=3$ transition here. States near 3.35 and 3.85 MeV reported as $(2f_{7/2})$ in Ref. 3 appear to be $(3p_{3/2})$ and $(3p_{3/2}, 1h_{9/2})$, respectively, in the present work.

The angular distributions for the $l=1$ transitions are shown in Fig. 5. The spectroscopic factors for the states near 3.42 and 4.06 MeV agree well with the lower-energy results.[3] The level at 3.482 MeV was not resolved from the 3.42-MeV peak in the earlier work and the level at 3.53 MeV assigned as $(3p_{3/2})$ before is probably populated by an $l=5$ transition.

Angular distributions for the peaks containing $(1h_{9/2})$ transitions are shown in Fig. 6. These states lie between 3.5 and 5.3 MeV where the level density is large and hence cleanly separated states are rare. For many cases components due to lower-l transfers complicate the (d,p) angular distributions and hence the present results depend heavily on the $(\alpha, {}^3\mathrm{He})$ measurements. Those cases where more than one l transfer was apparent were treated as doublets and there is more uncertainty in the results for such cases. The peaks interpreted as $h_{9/2}$ are large in the $(\alpha, {}^3\mathrm{He})$ spectrum, and hence must be due to either $l=5$ or $l=6$ transitions. For the large $(\alpha, {}^3\mathrm{He})$ peaks that appeared as single peaks in the (d,p) spectra also, the agreement with the (d,p) results is satisfactory. The peaks at 3.73, 4.93, 5.12, and 5.23 MeV were not as apparent in the (d,p) spectra, but there were enough counts within an $(\alpha, {}^3\mathrm{He})$ resolution width centered on each energy to agree with the $(\alpha, {}^3\mathrm{He})$ result. Since the agreement with the (d,p) results is satisfactory, the tentative assignment of $(1h_{9/2})$ has been made for these states. None of the $h_{9/2}$ transitions were reported in the earlier work.[3-5]

V. SPECTROSCOPIC-FACTOR SUMS AND SINGLE-PARTICLE ENERGIES

The sum of the spectroscopic factors for each subshell should be a measure of the nonoccupation U_j^2 of that subshell in the target nucleus:

$$U_j^2 = \sum_i S_j(i),$$

where $S_j(i)$ is the spectroscopic factor for the ith state and the sum is over all the levels of the subshell. The center of gravity for a subshell defined as

$$E_j' = \frac{\sum_i E_j^*(i) S_j(i)}{\sum_i S_j(i)},$$

where $E_j^*(i)$ is the excitation energy of the ith state, is related to the quasiparticle energies of

TABLE IV. Sums of spectroscopic factors and centers of gravity in comparison with the results of pairing theory (see Ref. 17). The numbers outside parentheses include only those states for which definite spin assignments were made. The values inside the parentheses are for all states analyzed, including those with tentative assignments.

	Experiment			Pairing theory			
				Set I (Kisslinger-Sorensen)		Set II	
nl_j	Number of transitions	$\sum_i S_j(i)$	E_j' (MeV)	U_j^2	$E_j - E_{11/2}$ (MeV)	U_j^2	$E_j - E_{11/2}$ (MeV)
$1h_{11/2}$	1	0.41	0.0	0.36	0.00	0.40	0.0
$2d_{3/2}$	1	0.44	0.026	0.48	−0.043	0.48	−0.031
$3s_{1/2}$	1	0.33	0.232	0.087	0.752	0.14	0.613
$1g_{7/2}$	1	0.047	1.377	0.056	1.163	0.095	0.981
$2d_{5/2}$	(3)	(0.129)	(1.509)	0.031	1.89	0.056	1.65
$2f_{7/2}$	4(14)	0.687 (1.13)	2.84 (3.39)				
$3p_{3/2}$	2(5)	0.44 (0.82)	3.43 (3.57)				
$1h_{9/2}$	(10)	(0.76)	(4.72)				

Kisslinger and Sorensen.[17] In pairing theory[17] the quasiparticle energies are given by

$$E_j = [(\epsilon_j - \lambda)^2 + \Delta^2]^{1/2},$$

and the nonoccupation probability is given by

$$U_j^2 = \tfrac{1}{2}[1 + (\epsilon_j - \lambda)/E_j],$$

where ϵ_j is the single-particle energy of the subshell, λ is the Fermi energy of the nucleus, and Δ is one half the "energy gap." The parameters used in these calculations are listed in Table III. Those given in Set I are the parameters calculated from the data and formulas of Ref. 17. Those in Set II are the same except that the value of $\Delta = 1.44$ MeV, obtained in Ref. 3, has been used. The parameters in Set III are identical to those in Set II except that $\epsilon_{1/2}$ has been arbitrarily increased to improve the agreement with experiment for the $s_{1/2}$ state.

The spectroscopic-factor sums and the experimental centers of gravity E_j' are given in Table IV. Since ^{124}Sn has 74 neutrons, it is only eight neutrons short of a closed shell. The first five subshells listed in Table IV should contain these eight holes. The number of holes observed, $\sum_j (2j+1)\sum_i S_j(i)$, where the sum over j is over the first five subshells, is 8.49. This is in good agreement with the expected value. The three higher subshells listed in Table IV belong to the next major shell and hence should be empty in the target. A spectroscopic-factor sum near unity should be obtained for these subshells. The table indicates that essentially all the $f_{7/2}$ and $p_{3/2}$ strength and nearly all the $h_{9/2}$ strength is located.

The predictions of pairing theory[17] for parameter Sets I and II (Table III) are also given in Table IV. The quasiparticle energies exceeded 1 MeV in all cases, so the differences in quasiparticle energies for each subshell and the $h_{11/2}$ subshell are listed for comparison with the centers of gravity E_j'.

Using the parameters from Kisslinger and Sorensen[17] (Set I) the energy for the $d_{3/2}$ level is predicted to be lower than the $h_{11/2}$, but both the experimental and theoretical numbers are near 0. The $s_{1/2}$ level is predicted to be at much higher energy than observed, while the agreement for the $g_{7/2}$ and $d_{5/2}$ levels is much better. The predicted nonoccupation probabilities agree well with experiment for the $h_{11/2}$, $d_{3/2}$, and $g_{7/2}$ subshells. The predicted values for the $s_{1/2}$ and $d_{5/2}$ subshells are much smaller than the experimental values.

Using parameter Set II, which is the Kisslinger-Sorensen parameters with Δ changed to 1.44 as taken from Ref. 3, the agreement is somewhat improved for the $s_{1/2}$ and $d_{5/2}$ subshells. However, it is poorer for the $g_{7/2}$ subshell. If the parameters are further changed to Set III, i.e., $\epsilon_{1/2}$ is changed from 1.28 to 2.0 MeV, the nonoccupation probability $U_{1/2}^2$ becomes 0.26 and $E_{1/2} - E_{11/2}$ becomes 0.169 in much better agreement with experiment. However, since a single nucleus is being considered, such adjustment of a single-particle energy is less meaningful than parameter searches involving large volumes of data, and hence searches were not made on the ϵ_j to obtain the best fit to the present data.

Better agreement between the $d_{5/2}$ spectroscopic-factor sum and the pairing-theory prediction can possibly be established through a different interpretation of the data. If the $d_{(5/2)}$ state at 1.277 MeV were interpreted as $d_{3/2}$, then $\sum_i S_{3/2}(i)$ and the $E_{3/2}'$ would be ~0.56 and 0.29 MeV, respectively, still in fair agreement with the pairing-theory predictions. The values for the $d_{5/2}$ subshell would then be 0.054 and 1.738 MeV, respectively. These are in much better agreement with the predictions of pairing theory.

ACKNOWLEDGMENTS

We are grateful to M. L. Halbert and B. D. Belt for their assistance in acquiring the data. The careful plate scanning of Barbara Monroe and Phyllis Wagner is gratefully acknowledged.

---

*Research supported by U. S. Army Research Office—Durham, under a grant to the University of Tennessee, and by the U. S. Atomic Energy Commission under contract with Union Carbide Corporation.

[1]C. R. Bingham and M. L. Halbert, Phys. Rev. C 2, 2297 (1970).

[2]C. R. Bingham and G. T. Fabian, Phys. Rev. C 7, 1509 (1973).

[3]E. J. Schneid, A. Prakash, and B. L. Cohen, Phys. Rev. 156, 1316 (1967).

[4]B. L. Cohen and R. E. Price, Phys. Rev. 121, 1441 (1961).

[5]C. L. Nealy and R. K. Sheline, Phys. Rev. 135, B325 (1964).

[6]D. L. Powell, P. J. Dallimore, and W. F. Davidson, Aust. J. Phys. 24, 793 (1971).

[7]E. Newman, L. C. Becker, B. M. Preedom, and J. C. Hiebert, Nucl. Phys. A100, 225 (1967).

[8]M. P. Fricke, E. E. Gross, B. J. Morton, and A. Zucker, Phys. Rev. 156, 1207 (1967).

[9]C. R. Bingham, M. L. Halbert, and A. R. Quinton, Phys. Rev. 180, 1197 (1969).

[10]C. R. Bingham and M. L. Halbert, Phys. Rev. C 1, 244 (1970).

[11]Program developed by R. M. Drisko, R. H. Bassel, and G. R. Satchler.
[12]C. R. Bingham and M. L. Halbert, Phys. Rev. 158, 1085 (1967).
[13]F. G. Perey and A. M. Saruis, Nucl. Phys. 70, 225 (1965).
[14]J. K. Dickens, R. M. Drisko, F. G. Perey, and G. R. Satchler, Phys. Lett. 15, 337 (1965).
[15]C. R. Bingham, M. L. Halbert, and R. H. Bassel, Phys. Rev. 148, 1174 (1966).
[16]E. F. Gibson, B. W. Ridley, J. J. Kraushaar, M. E. Rickey, and R. H. Bassel, Phys. Rev. 155, 1194 (1967).
[17]L. S. Kisslinger and R. A. Sorensen, Rev. Mod. Phys. 35, 853 (1963).